

## NEW CRATERS ON MARS: RESULTS FROM A COMPLETE CATALOG OF 1,203 RECENT IMPACTS.

Ingrid J. Daubar<sup>1</sup>, C. Dundas<sup>2</sup>, A. S. McEwen<sup>3</sup>, A. Gao<sup>1</sup>, D. Wexler<sup>1</sup>, S. Piqueux<sup>4</sup>, G. S. Collins<sup>5</sup>, K. Miljkovic<sup>6</sup>, T. Neidhart<sup>6</sup>, J. Eschenfelder<sup>5</sup>, G. D. Bart<sup>7</sup>, K. Wagstaff<sup>4</sup>, G. Doran<sup>4</sup>, L. Posiolova<sup>8</sup>, G. Speth<sup>8</sup>, D. Susko<sup>8</sup>, A. Werynski<sup>8</sup>, M. Malin<sup>8</sup>. <sup>1</sup>Brown University, Providence, RI, USA (ingrid\_daubar@brown.edu). <sup>2</sup>USGS, Flagstaff, AZ, USA. <sup>3</sup>University of Arizona, Tucson, AZ, USA. <sup>4</sup>Jet Propulsion Laboratory, California Institute of Technology, Pasadena, CA, USA. <sup>5</sup>Imperial College, London, UK. <sup>6</sup>Curtin University, Perth, Australia. <sup>7</sup>University of Idaho, Moscow, ID, USA. <sup>8</sup>Malin Space Sciences Systems, San Diego, CA, USA.

**Introduction:** Newly formed craters were first discovered on Mars using the Mars Orbiter Camera [1], a process which has continued with the Context Camera (CTX) [2,3]. These new craters have provided valuable new information about Mars, including the present-day cratering rate [2], shallow subsurface ice [4–6], and mineralogy under dust cover [7]. The statistics [2,8,9], morphologies [10], and some of the albedo features [11–13] around the new craters have been studied. Clusters have been used to investigate atmospheric fragmentation processes [14–17]. Current martian cratering is also of special interest to the InSight mission as a potentially important, although as yet unrecognized, source of seismic signals of known size and location [18–22].

A comprehensive catalog of current cratering on Mars is important because: (1) Larger impacts are rarer, so a longer temporal baseline results in more large impacts and extends our knowledge of the crater size-frequency distribution (SFD) to larger sizes. (2) Larger impacts are less affected by atmospheric ablation and deceleration, thus reflecting the primary impacting population more accurately. (3) Improved impact statistics, especially of features that are rarer. (4) Extended areal coverage better constrains e.g. latitude trends. (5) A better understanding of observational biases, including the effects of different target materials.

**Catalog contents:** We report crater diameters for all impacts in this catalog [3], and for each cluster impact site an effective diameter ( $D_{\text{eff}} = \sqrt[3]{\sum_i D_i^3}$ , where  $D_i$  is the diameter of the individual craters within the cluster [1,23]). We list information about the constraining (before and after) images, whether the impact is a single crater or a cluster, and exposed subsurface ice. These albedo features are also included in the catalog (Fig. 1):

*Halos:* An area of contrasting albedo with a diffuse edge with a circular to sub-circular shape around the impact site (Fig. 1, middle and right columns). Halos are a few to hundreds of times larger than the crater itself [13], and are the most helpful features for identifying small, new craters in lower resolution images.

*Linear Rays:* Sharply defined linear features that extend outward from the center of the crater (Fig. 1, left and right columns).

*Arcuate Rays:* Curved paths outwards from the impact site (Fig. 1c).

*Blast zone albedo:* While most albedo features are

darker than the surroundings (Fig. 1d, e, g, i), some craters have light-toned (Fig. 1f) or dual-toned blast zones (Fig. 1b, h).

**Results:** Our catalog includes 1,203 impact sites ranging from 1 to 58 meters in (effective) diameter, all of which have formed within the last few decades [3]. Formation time periods are constrained by available images to windows that range from one day to 33 Earth years long, averaging 4.5 Earth years. Diffuse halos and linear rays are the most common features around new impacts; arcuate rays are not common. Most blast zones are dark relative to the surroundings, with rare light- and dual-toned blast zones. We see no apparent trend with elevation or size in the occurrence of clusters as compared to single-crater impacts. The albedo features we observe (halos, arcuate rays, and their relative tones) have no dependence on whether the impact is a single or cluster of craters. From this we conclude that the formation mechanisms of these features do not obviously depend on atmospheric fragmentation.

Halos appear to be related to atmospheric pressure; we conclude their formation is related to impact airbursts. Linear rays seem to form by impact into and/or ejection of material with higher strength, such as would be encountered by larger impacts into deeper and thus more consolidated target material. Higher impact velocities and/or ejecta traversing through more tenuous atmosphere at higher elevations could also favor rays.

The catalog shows an uneven distribution of impacts with respect to surface thermal inertia, with a strong bias towards areas of lower thermal inertia. This has implications for the type of target material the features around new impacts form in: highly mobile, dust-like surficial material, readily displaceable at the time of the impact by the blast, favors the formation of detectable albedo changes. The presence of bright surface dust is necessary but not sufficient to explain the observed distribution; a lack of cohesion or induration is also needed to form the observed features.

Rarer light-toned blast zones occur mostly in specific regions,  $-15^\circ$  to  $-45^\circ$  latitude in areas corresponding to higher thermal inertia. Larger impacts are more likely to have dual- and light-toned BZs, indicating that they are formed from the excavation of material at  $\sim 0.5$ -1 m depth, rather than merely a surficial disturbance or deposition of impactor material.

Compared to the limited dataset using only CTX-CTX-constrained impacts, the size frequency

distribution (SFD) slope of these new impacts is steeper at larger sizes, with a larger-diameter resolution rollover. This is likely due to the use of datasets with lower resolution in the date-constraining discovery images, resulting in fewer smaller craters. The slope of the differential SFD for craters larger than 8 m diameter is 2.9 (cumulative slope 2.2), which is close to previously published models [24]. However, we continue to caution against using craters in this size range (meters-tens of meters) to estimate surface exposure ages of older surfaces, and we caution against extrapolating this SFD to even smaller sizes.

The SFD slope for this dataset is shallower than that of new lunar impacts reported by [25]. Accounting for known biases in our dataset (surface properties affecting detection, resolution of detection cameras, higher detection rates in areas of low thermal inertia, and size-dependent fading over time) does result in steeper SFDs, but still not as steep as that seen on the Moon. Differences in impacting populations, target properties, or atmospheric effects do not easily explain the difference in slope, either. Although we cannot yet explain the dif-

ference in SFD slopes between modern Mars and the Moon, we believe that no systematic biases exist in the martian dataset sufficient to explain the discrepancy.

**References:** [1] Malin et al. (2006) *Science* **314**, 1573–1577. [2] Daubar et al. (2013) *Icarus* **225**, 506–516. [3] Daubar et al. (2022) *JGRP* in review. [4] Byrne et al. (2009) *Science* **325**, 1674–6. [5] Dundas et al. (2014) *JGRP* **119**, 109–127. [6] Dundas et al. (2021) *JGRP* **126**, 1–28. [7] Viviano et al. (2019) *Icarus* **328**, 274–286. [8] Williams et al. (2014) *Icarus* **235**, 23–36. [9] Hartmann & Daubar (2017) *MAPS* **52**, 493–510. [10] Daubar et al. (2014) *JGRP* **119**, 2620–2639. [11] Burleigh et al. (2012) *Icarus* **217**, 194–201. [12] Daubar et al. (2016) *Icarus* **267**, 86–105. [13] Bart et al. (2019) *Icarus* **328**, 45–57. [14] Daubar et al. (2019) *JGRP* **124**, 10.1029/2018JE005857. [15] Newland et al. (2019) *LPSC 50* Abs. 2569. [16] Neidhart et al. (2022) *JGRP* in review. [17] Collins et al. (2022) *JGRP* in review. [18] Teanby & Wookey (2011) *PEPI* **186**, 70–80. [19] Teanby (2015) *Icarus* **256**, 49–62. [20] Stevanović et al. (2017) *SSR* **211**, 485–500. [21] Daubar et al. (2018) *SSR* **214**, 132. [22] Daubar et al. (2020) *JGRP* **125**, e2020JE006382. [23] Ivanov et al. (2009) *LPSC Abstr.* 1410. [24] Hartmann (2005) *Icarus* **174**, 294–320. [25] Speyerer et al. (2016) *Nature* **538**, 215–218.

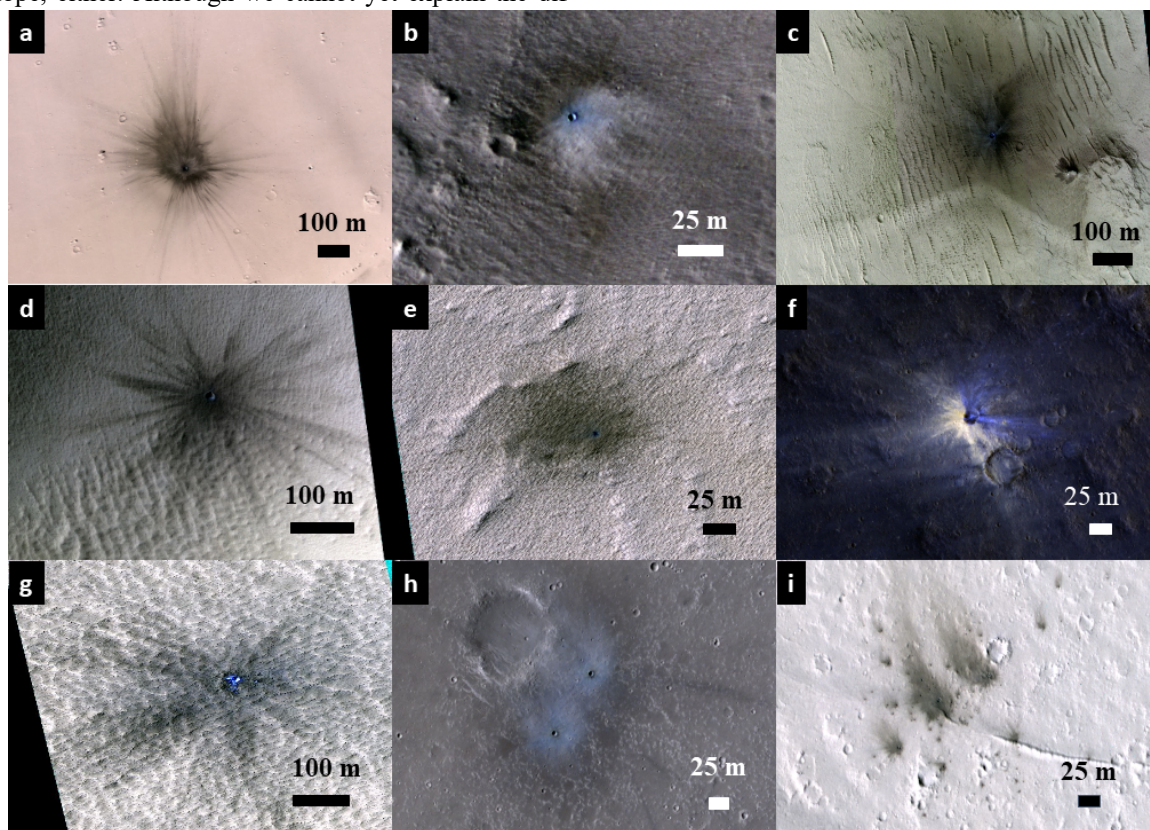


**Figure 1.** Albedo features around new dated impacts on Mars. Row 1: dual-toned single craters; (a) ESP\_048888\_1735: linear rays and a halo; (b) ESP\_037544\_2060: halo; (c) ESP\_031965\_2050: halo, linear, and arcuate rays. Row 2: single craters; (d) ESP\_062128\_1725: dark-toned linear rays; (e) ESP\_017821\_1820: dark-toned halo; (f) ESP\_030566\_1860: light-toned linear rays and a diffuse halo. Row 3: clusters of craters; (g) ESP\_016954\_2245: exposed ice and dark-toned linear rays; (h) ESP\_053006\_1980: dual-toned blast zone, halos, rays; (i) ESP\_047175\_1955: dark-toned blast zone, halos, rays. The left column have rays, the middle column have halos, and the right column have rays as well as halos. Images are from HiRISE enhanced-color RDRs, stretched for contrast, with North up. Image credit: NASA/JPL/U of A.